Progress on Nonlinear Resistive MHD Code Verification Problems with M3D-C1

S. C. Jardin, N. Ferraro, J. Breslau, S. Hudson,
D. Pfefferle, B. Tobias, M.Lanctot

April 3-6 2016

Madison, Wisconsin

abstract

We report on progress in using the M3D-C1 code to perform several resistive MHD code verification problems for comparison with analytic solutions and other codes. The first set of problems was proposed by the ITPA group on control, MHD, and disruptions and is known as Joint Activity 2, or simply JA-2. The intent is to study the interaction of several tearing modes in a torus. As a prelude to that, we have performed linear and non-linear analysis of two low-beta configurations that are unstable to one or more tearing modes. Configuration (1) has an analytic q-profile given (in cylindrical geometry) by: $q(r) = 1.15 \times (1 + (r^2/.6561))$ and is unstable to only the (2,1) mode. Configuration (2) has q-profile: $q(r) = 1.33 \times (1 + (r^2/.354)^4)^{1/4}$ (also in cylindrical geometry) and is unstable to both the (2,1) and (3,2) modes. For each of these configurations, we have also defined axisymmetric toroidal equilibrium that have the same $q(\psi)$ profiles (where ψ is the normalized poloidal flux) for comparison. The second set of problems came from discussions over the last year at both the "Transients in Tokamak Plasmas" and "Integrated Simulations" workshops. For these, besides the plasma region we include vacuum regions, resistive wall, and in some apply externally imposed "error fields" to study the evolution of tearing modes in the presence of more realistic and complex boundary conditions.

Outline

1. Linear resistive MHD test problems for JA-2

2. Nonlinear resistive MHD test problems for JA-2

3. Nonlinear resistive MHD test problem with resistive wall and error fields

Outline

1. Linear resistive MHD test problems for JA-2
2. Nonlinear resistive MHD test problems for JA-2
3. Nonlinear resistive MHD test problem with resistive wall and error fields

Progress on ITPA JA-2 benchmark with M3D-C1

- We started with a cylindrical equilibrium with a given q(r) profile. This was then converted to a toroidal A=10 equilibrium with the same q(ψ). This was unstable to both n=1 and n=2 modes.

$$q(r) = 1.33\left[1 + \left(r^2/.354\right)^4\right]^{1/4}$$

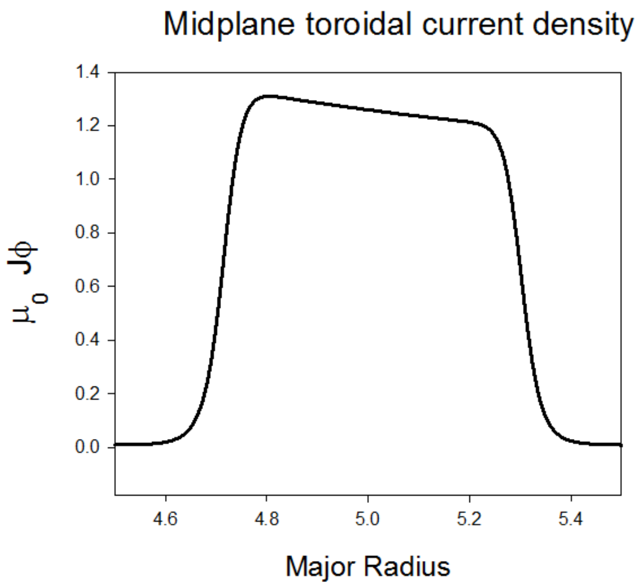

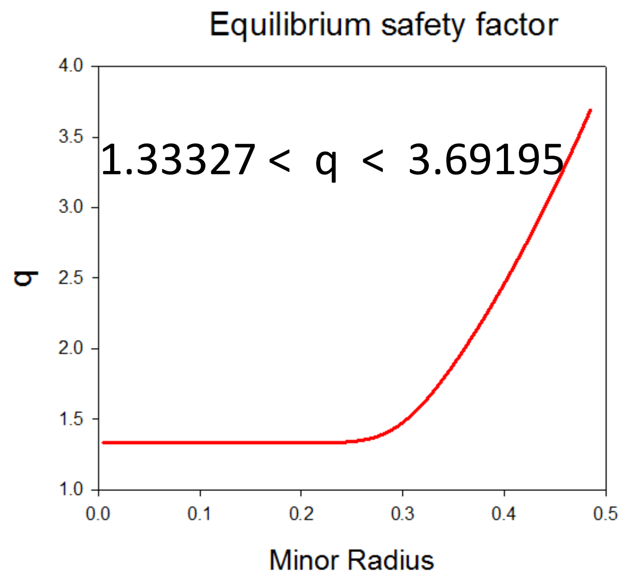

Equilibrium parameters (SI units): R=5, a=0.5, B_T = 4.2, $n_0 = 10^{20}$

$$\eta = 0.21\times10^{-6}\eta_0, \qquad \nu = 10^{-8}\nu_0, \qquad t_0 = \left[\mu_0 n_0 M_i\right]^{1/2} = 4.58\times10^{-7}$$

$$\eta_0 = \left[\frac{\mu_0}{n_0 M_i}\right]^{1/2} = 7.52, \qquad \nu_0 = \left[\frac{n_0 M_i}{\mu_0}\right]^{1/2} = 0.132, \qquad S \equiv \frac{a^2 B_T}{R}\frac{\eta_0}{\eta} = 10^6$$

2. Normal displacement and perturbed current eigenfunctions for n=1 mode

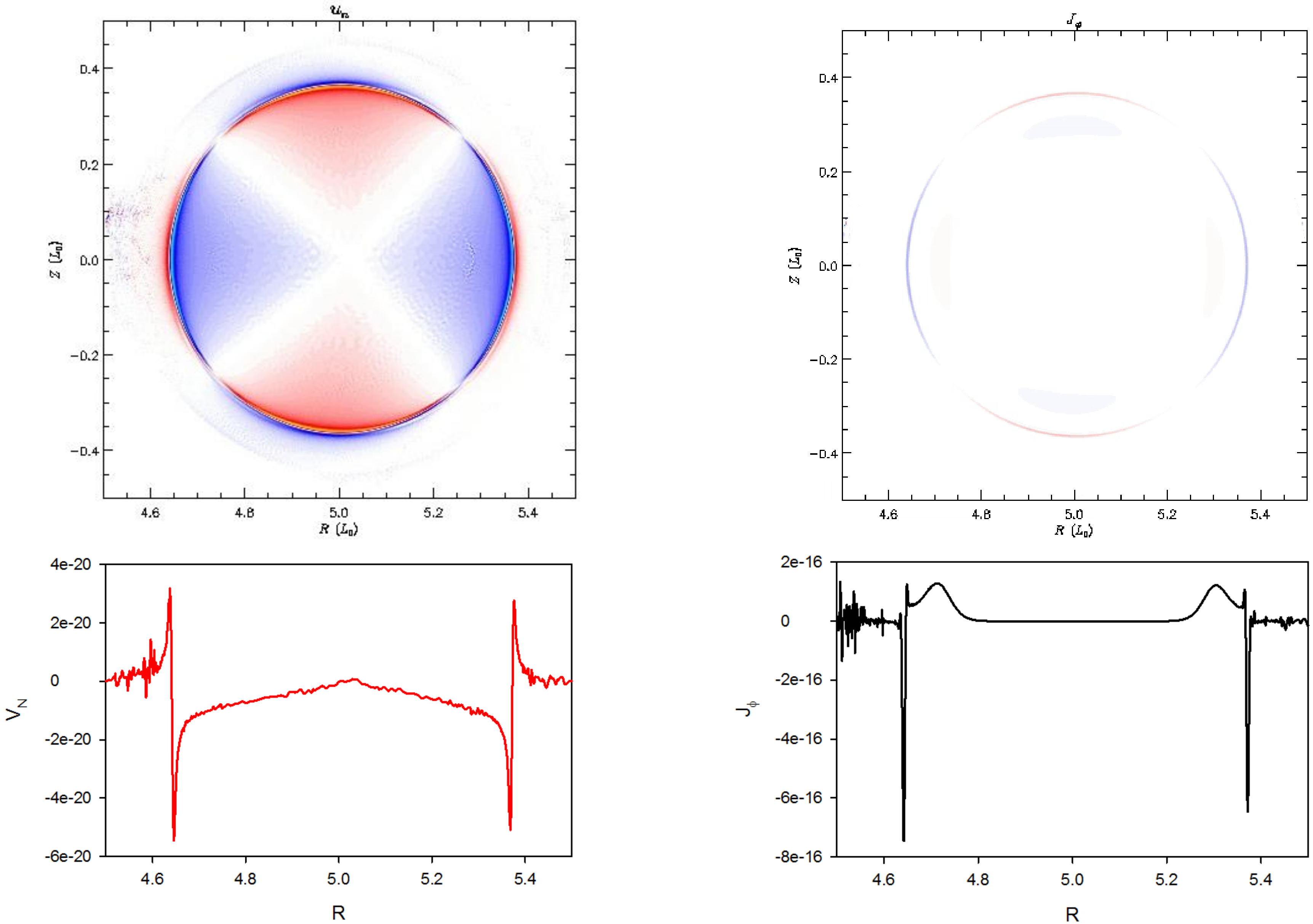

3. Normal displacement and perturbed current eigenfunctions for n=2 mode

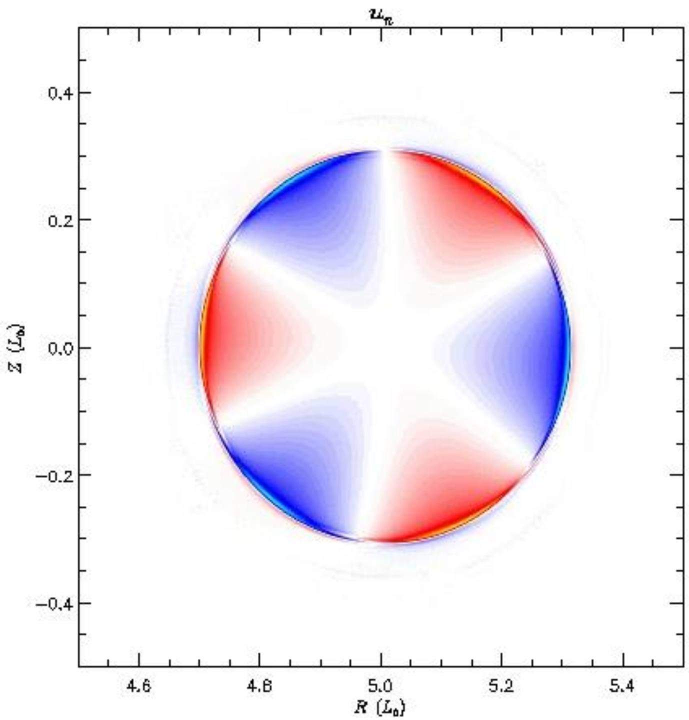

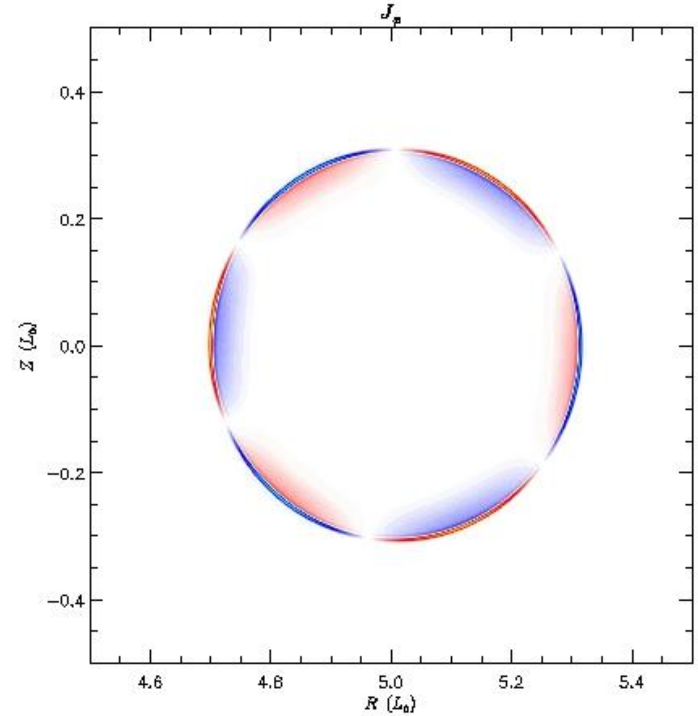

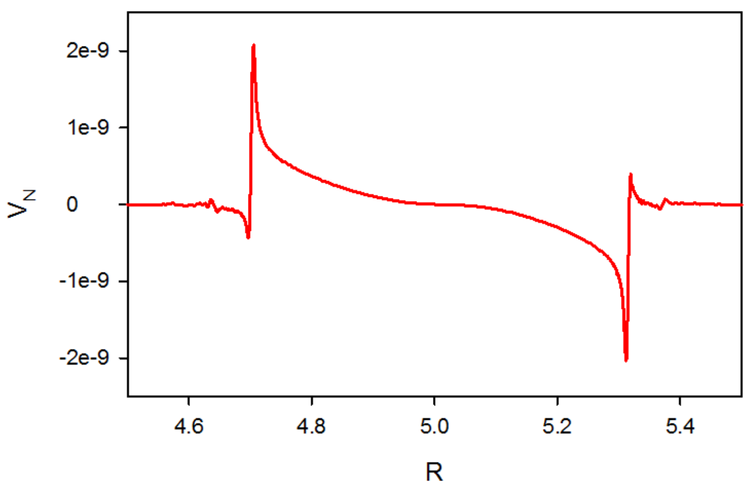

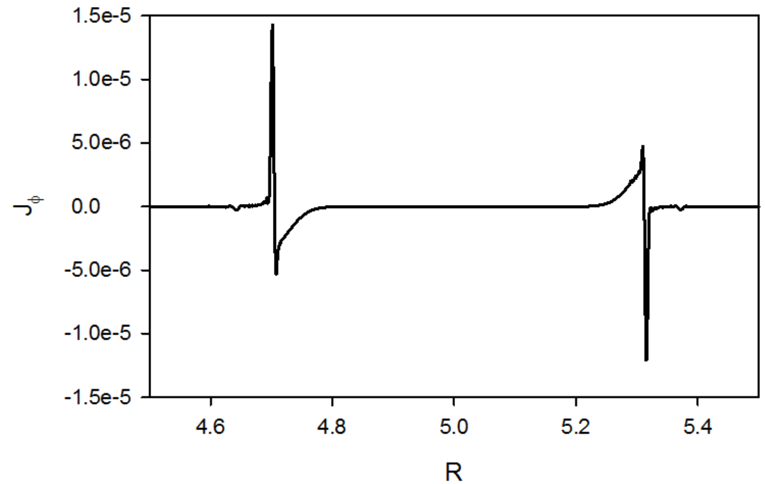

4. Adapted mesh used for n=1 mode

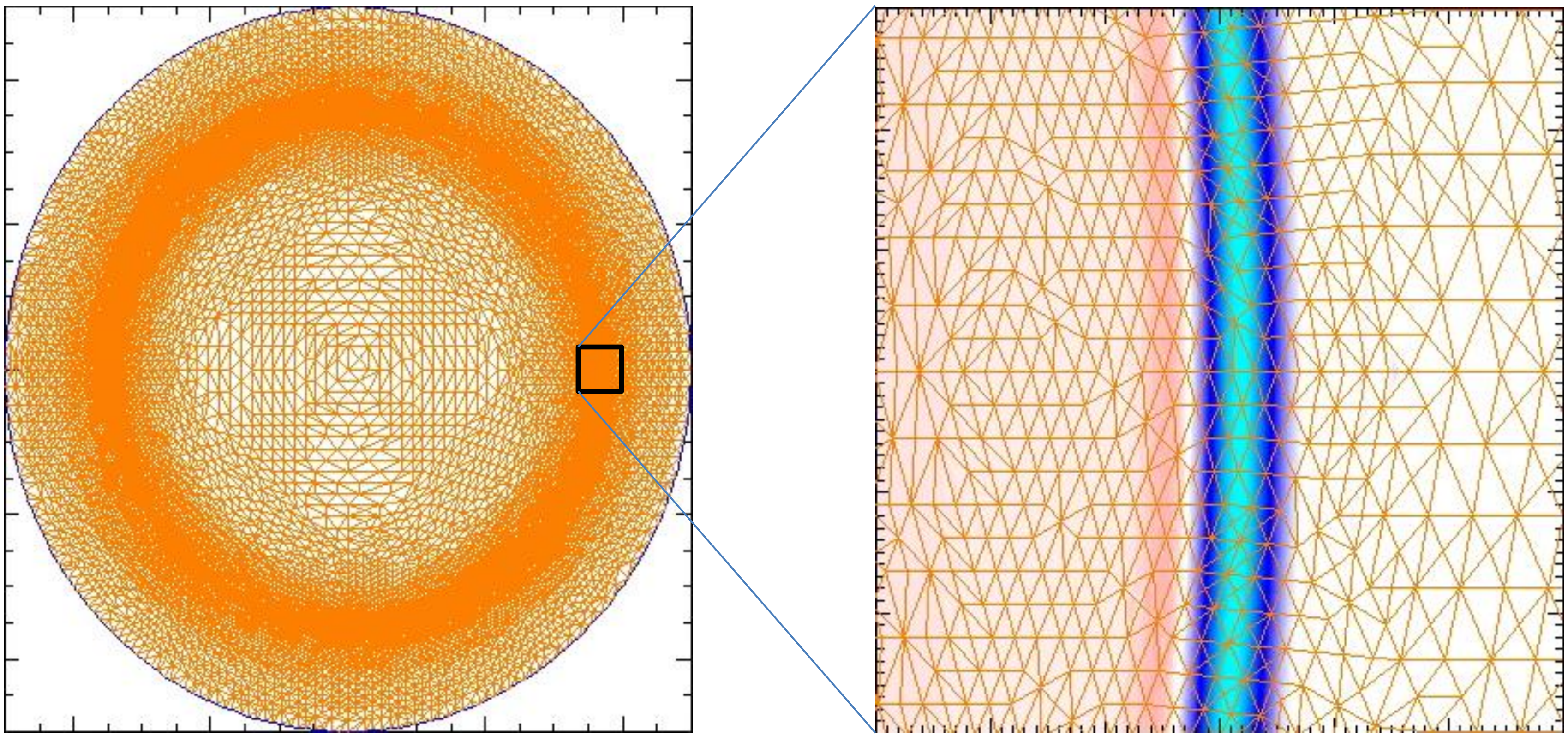

Mesh size varies from 0.002 to 0.03

5. Adapted mesh used for n=2 mode

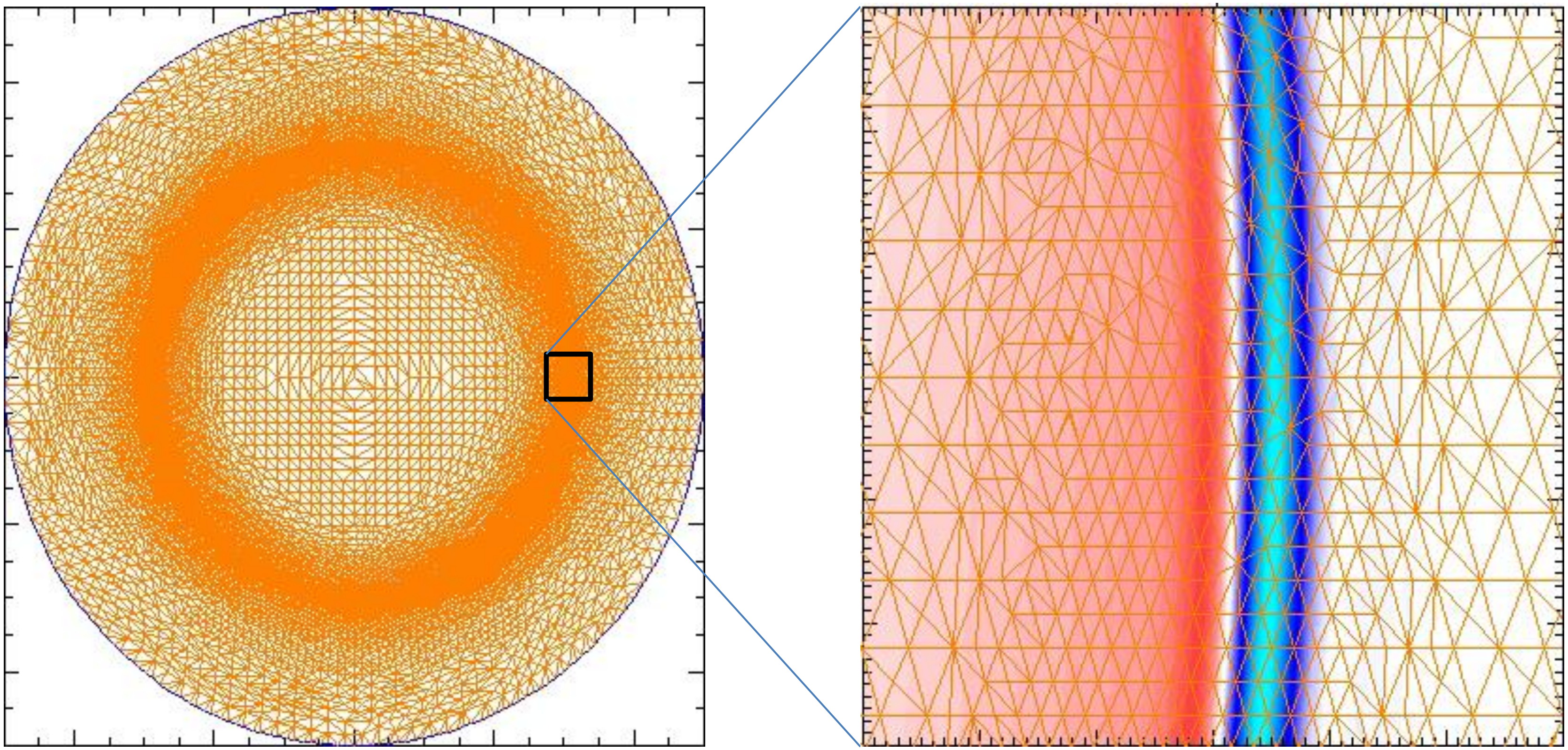

Mesh size varies from 0.002 to 0.03

6. Convergence study for the $S=10^6$, $\beta=0$, A=10 equilibrium

DT	ΔX_{min}	$\gamma_{n=1} t_H$	$\gamma_{n=2}\, t_H$
5 τ_A	0.002	**1.64 E-3**	**7.19 E-3**
5 τ_A	0.004	1.70 E-3	7.87 E-3
10 τ_A	0.002	1.65 E-3	7.29 E-3

$$\tau_H \equiv \frac{R}{B_T}\left[\mu_0 n_0 M_i\right]^{1/2}$$

7. Dependence on geometry and beta

n=1

geom	β	$\gamma\tau_H$
A=10	0	1.64 E-3
A=10	10^{-6}	1.13 E-3
Cyl	0	1.49 E-3
Cyl	10^{-6}	1.49 E-3

n=2

geom	β	$\gamma\tau_H$
A=10	0	7.19 E-3
A=10	10^{-6}	5.00 E-3
Cyl	0	2.89 E-3
Cyl	10^{-6}	2.00E-3

- n=2 is always more unstable than n=1
- Finite pressure is stabilizing in torus, not so much in cylinder
- Toroidal geometry is more unstable than cylinder, especially for n=2

8. Test of growth rate with different numerical options:

Cylindrical test case:

p_0 = 1.E-4, dt = 2.0, μ = 1.e-5, η =1.e-5 (S = 2.1 x 10^4), uniform mesh $\Delta x \sim 0.03$

isplitstep=1							isplitstep=0
	impmod=0			impmod=1			
	16	32	linear	16	32	linear	linear
n=1	.0063	.0063	.0063	.0070	.0070	.0071	.0072
n=2	.0048	.0048	.0048	.0064	.0064	.0064	.0066

Conclusions:

1. isplitstep=0 is most accurate, but only viable for linear runs
2. impmod = 1 (Caramana advance) more accurate than impmod=0
3. Good convergence in toroidal mode number for low-n modes (1 and 2)

For explanation of impmod=0,1, see: Ferraro and Jardin, JCP 228 (2009) 7742-7770

Linear Benchmarking

Cylindrical $q=1.33(1 + (r/0.595)^8)^{0.25}$ and $\beta=0$

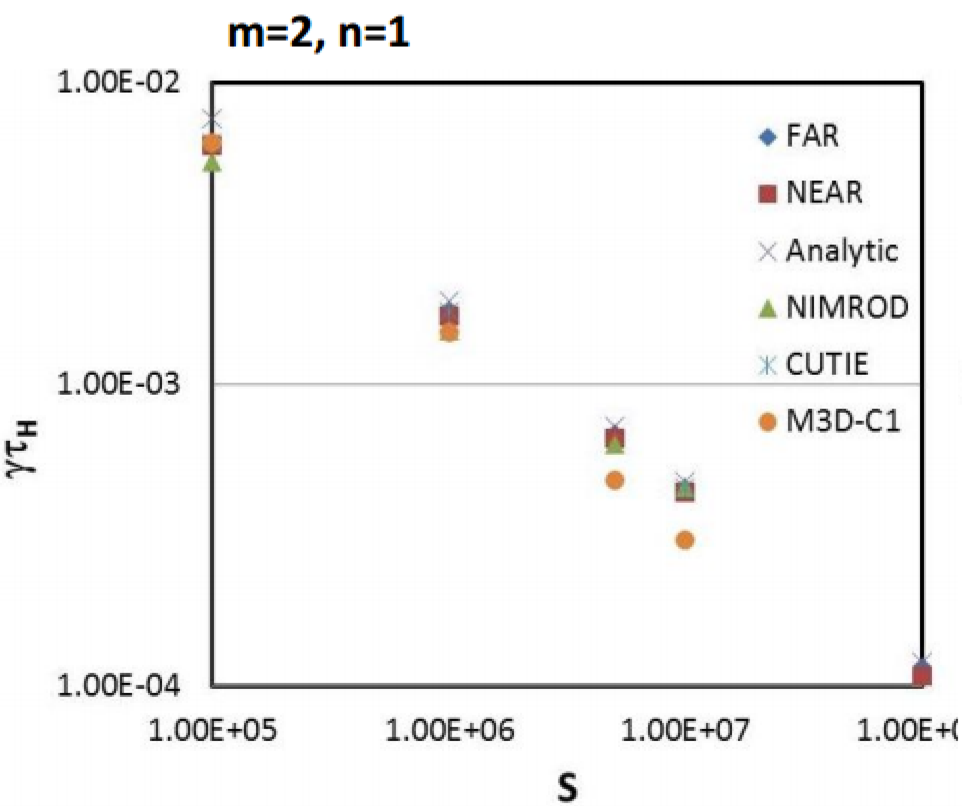

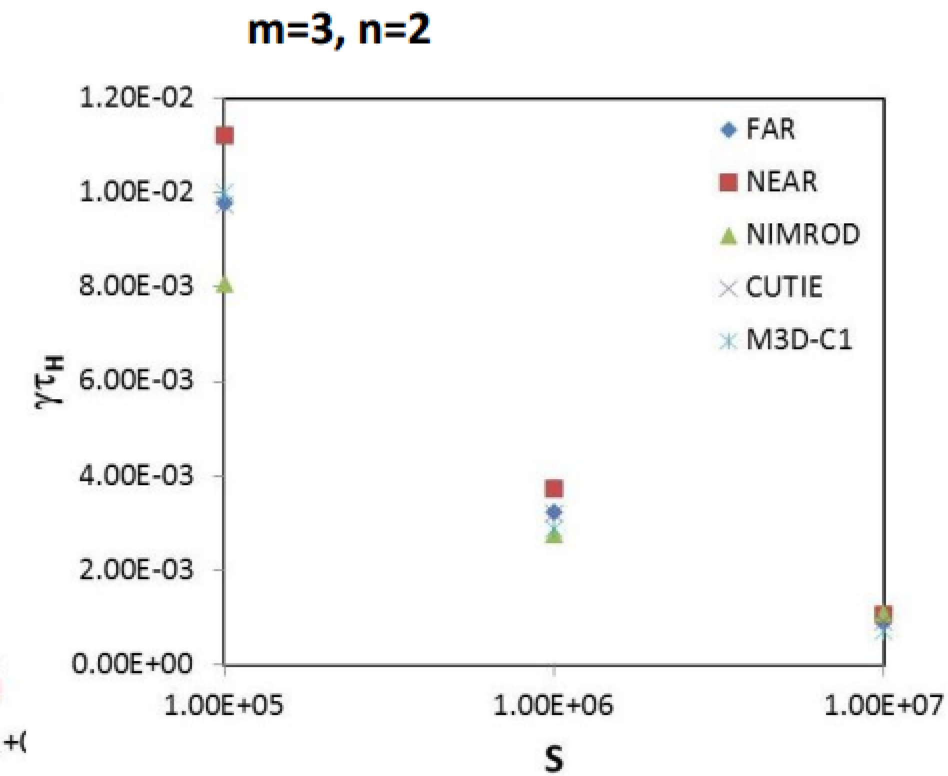

Linear Benchmarking

R/a=10, $q=1.33(1 + (r/0.595)^8)^{0.25}$ and $\beta_0=1.1\times10^{-7}$

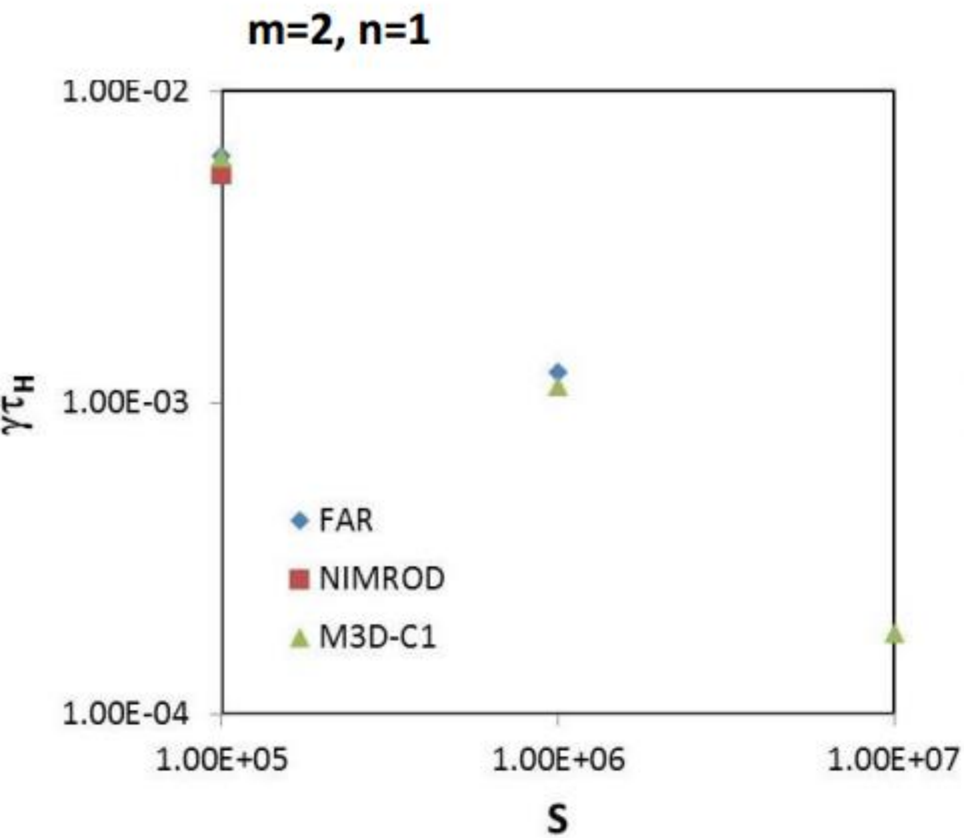

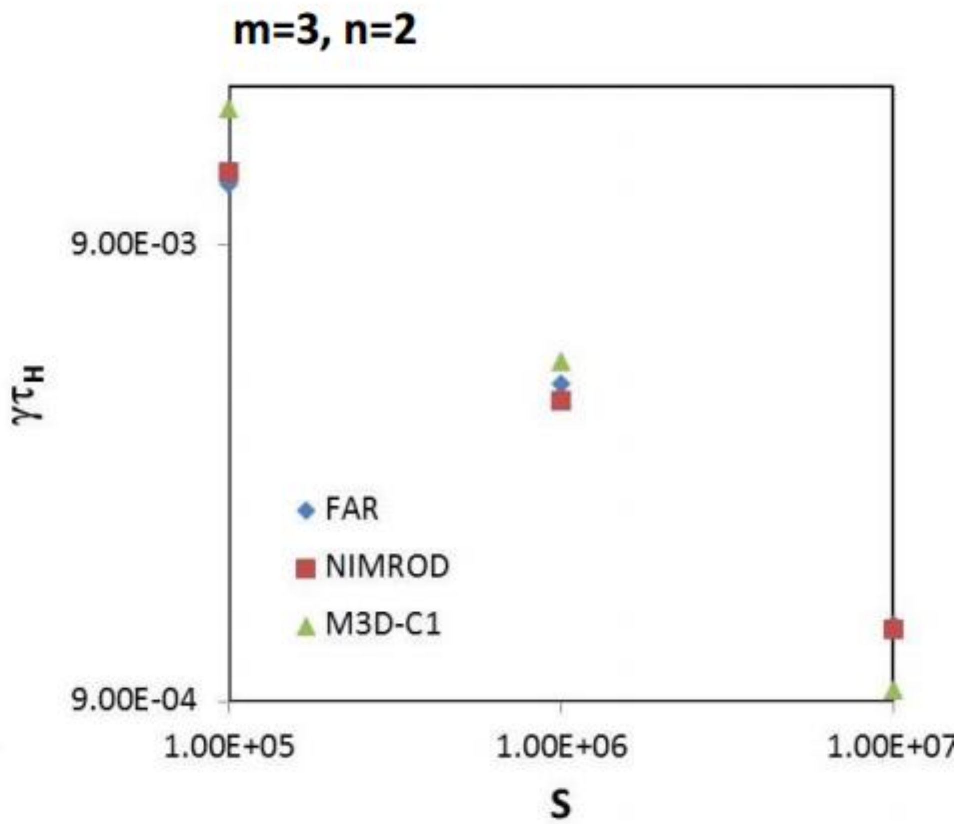

Outline

1. Linear resistive MHD test problems for JA-2
2. Nonlinear resistive MHD test problems for JA-2
3. Nonlinear resistive MHD test problem with resistive wall and error fields

Non-Linear Runs looked at Two Equilibria

$$q(r) = 1.33\left[1+\left(\frac{r^2}{.354}\right)^4\right]^{1/4}$$

- **Two-Mode** Case (same as linear)
- n=1 and n=2 unstable
- Cylinder, A=3, A=10 torus
- Linear and Nonlinear

$$q(r) = 1.15\left[1+\left(\frac{r^2}{.6561}\right)\right]$$

- **One-Mode** Case
- Only n=1 unstable
- Cylinder, A=3, A=10 torus
- Linear and Nonlinear

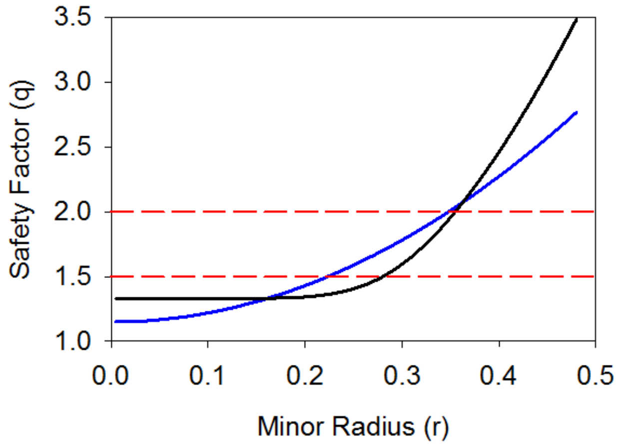

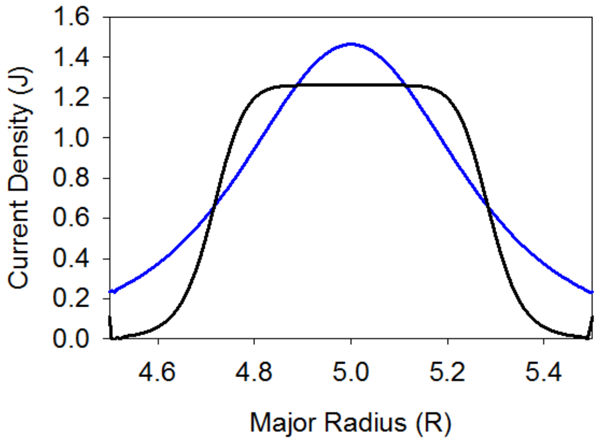

Non-Linear Results

1. **Two-Mode case: Ran Nonlinear A=10 Torus numvar=3**
   - $S = 2 \times 10^4$ $\nu/\eta = 1$
   - Ran both 32 and 16 toroidal planes (with hermit cubic elements)

In both cases, islands continue to grow and becomes totally stochastic by Time Slice 30. (t=1500) Very similar results for N=16 and N=32 plane cases. Error α N^4

2. **One-Mode Case**: Ran Cylindrical geometry case to saturation with reduced MHD
   - $S = 10^5$, $\nu/\eta = .047$

Much slower island growth than above. Island saturates at about W/a = .14 at t=50,000

- Now running A=10 toroidal cases with full MHD

Mode Growth vs time for **Two-mode case**

Comparison of 16 planes (solid) and 32 planes (dashed)

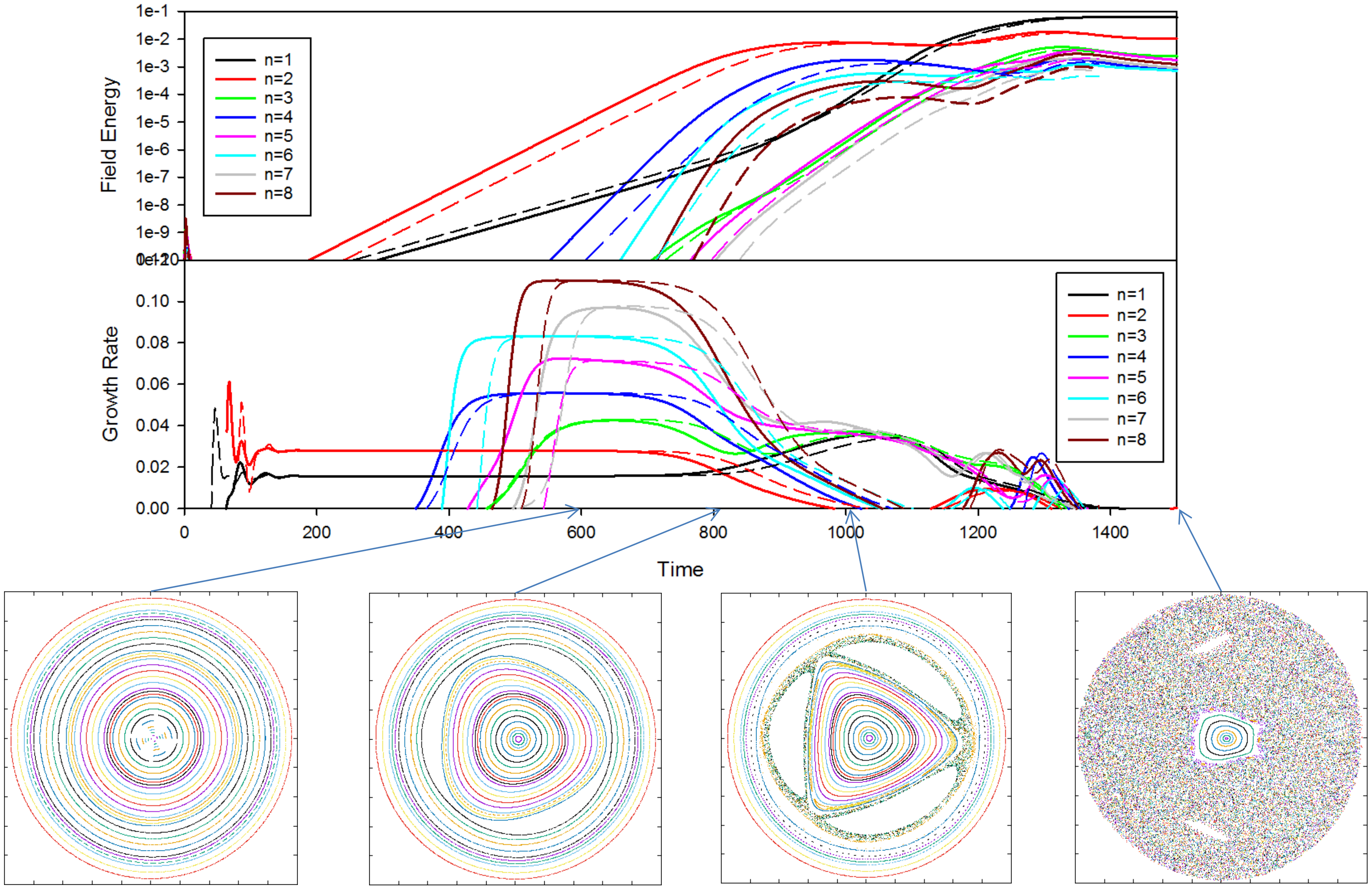

Comparison of surfaces at time t=1200 for **Two-Mode case** with 16 and 32 Planes

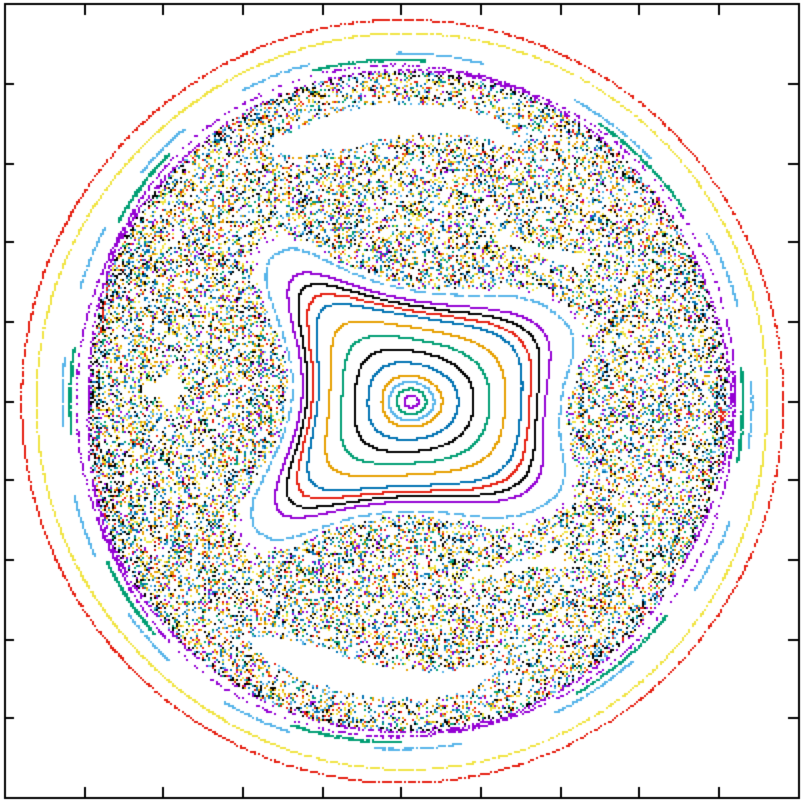

16 Planes

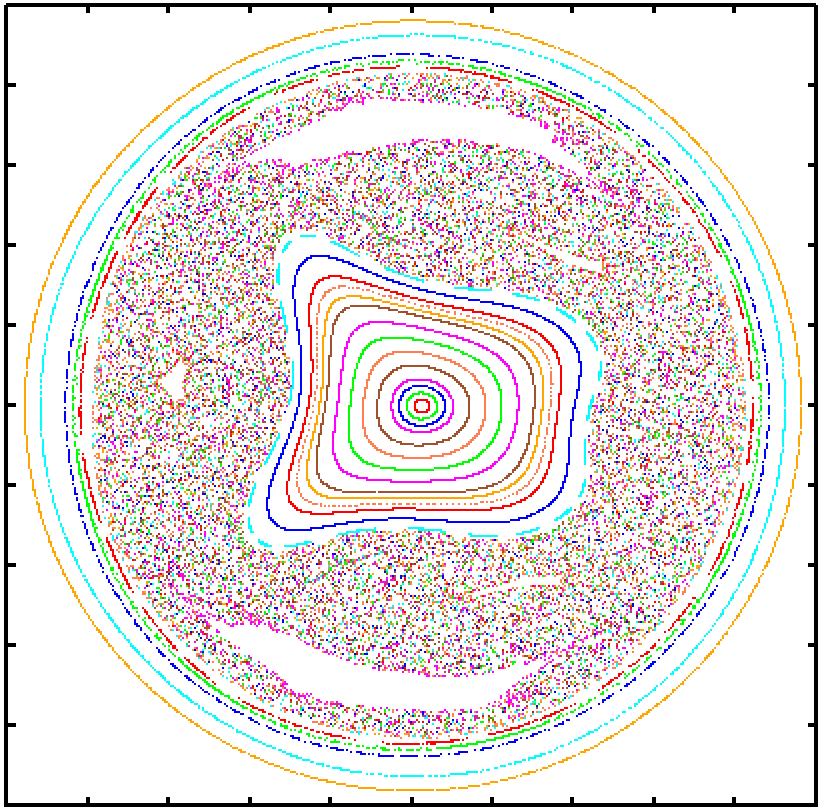

32 Planes

Single Unstable Mode Case in a cylinder

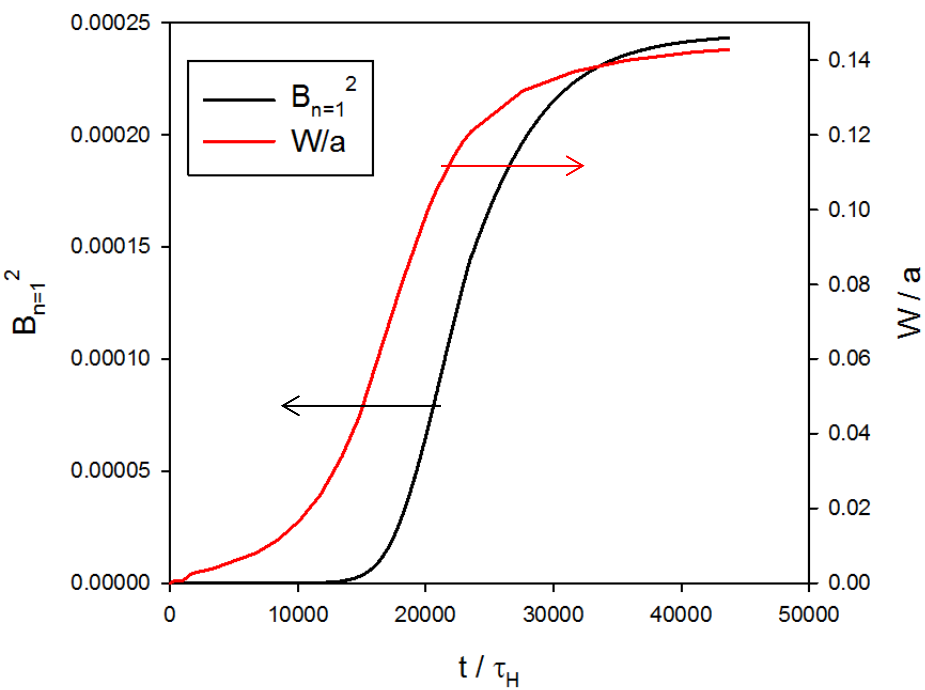

Island width and magnetic energy in n=1 harmonic vs time.

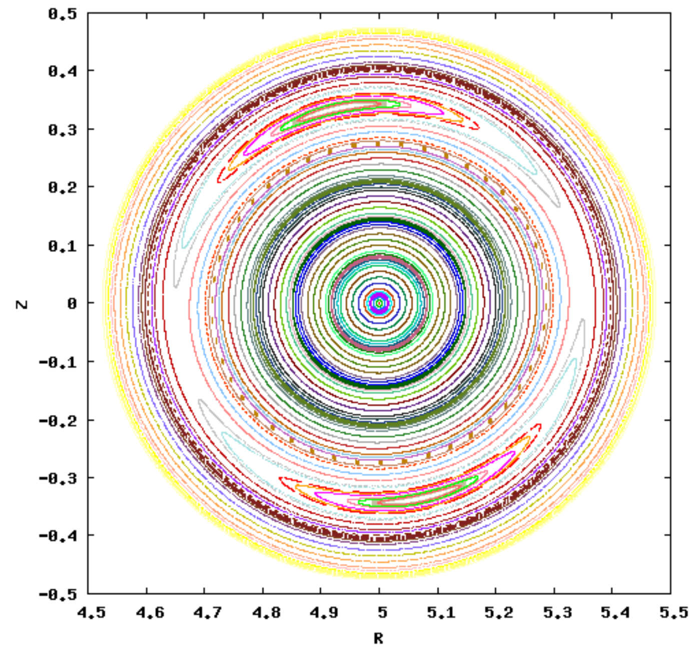

Poincare plot at final time.

$$q(r) = 1.15\left[1 + \left(\frac{r}{0.81}\right)^2\right]$$

SI Units: R=5, a=0.5, B_T = 4.2, n_0 = 10^{20}

$$S = \frac{a^2 B_T}{\eta R}\left[\frac{\mu_0}{n_0 M_i}\right]^{1/2} = 10^5, \quad \tau_H \equiv \frac{R}{B_T}\left[\mu_0 n_0 M_i\right]^{1/2}, \quad \nu/\eta = .047$$

N=0 (axisymmetric) equilibrium not advanced in time.

Low $\beta < 10^{-7}$

/tigress/sjardin/JA-2/One_Mode/Cylinder

Outline

1. Linear resistive MHD test problems for JA-2
2. Nonlinear resistive MHD test problems for JA-2
3. Nonlinear resistive MHD test problem with resistive wall and error fields

Model Cylindrical Equilibrium

- Poloidal flux low order polynomial in r^2
- Current density vanishes at a
- $q_0 < q < q_a$

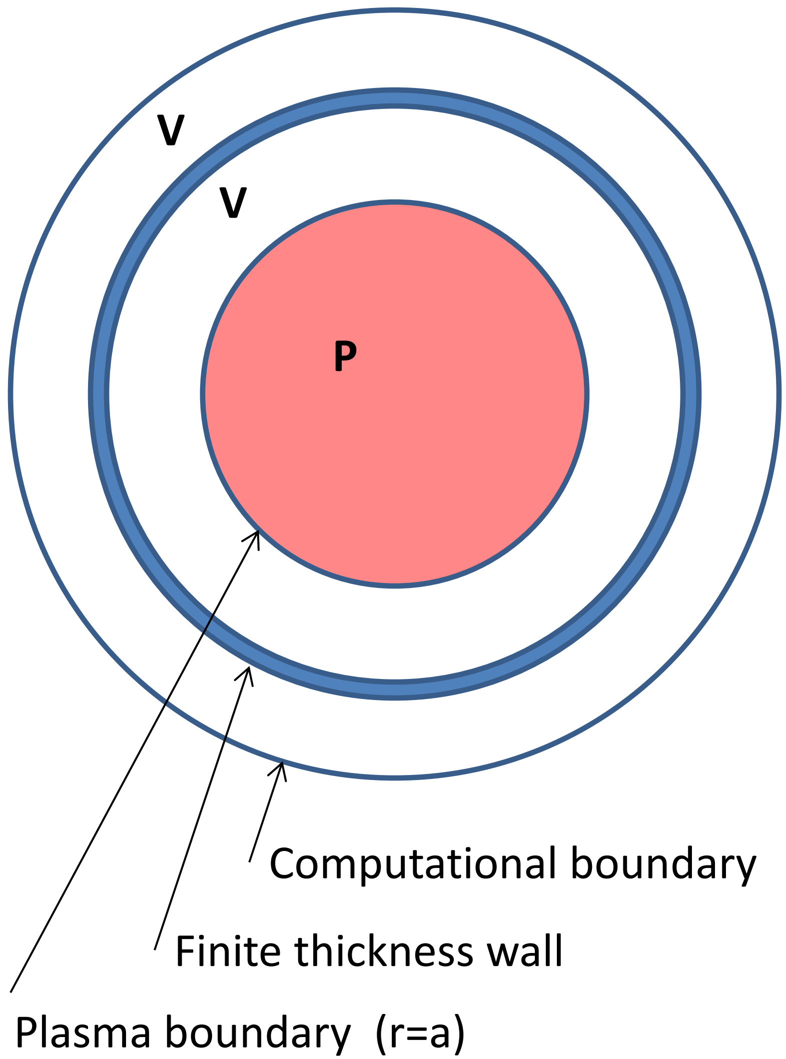

$$\Psi(r)=\begin{cases}\dfrac{B_T r^2}{2q_0 R}\left[1-(r/a)^2\left(1-\dfrac{3}{2}\dfrac{q_0}{q_a}\right)+\dfrac{1}{3}(r/a)^4\left(1-2\dfrac{q_0}{q_a}\right)\right] & r<a\\ \dfrac{a^2 B_T}{6q_0 R}\left[1+\dfrac{5}{2}\dfrac{q_0}{q_a}+6\dfrac{q_0}{q_a}\ln(r/a)\right] & r\geq a\end{cases}$$

$$J(r)=\frac{B_T}{6q_0 R}\left[1-4(r/a)^2\left(1-\frac{3}{2}\frac{q_0}{q_a}\right)+3(r/a)^4\left(1-2\frac{q_0}{q_a}\right)\right]$$

$$q(r)=\begin{cases}q_0\left[1-2(r/a)^2\left(1-\dfrac{3}{2}\dfrac{q_0}{q_a}\right)+(r/a)^4\left(1-2\dfrac{q_0}{q_a}\right)\right]^{-1} & r<a\\ q_a(r/a)^2 & r\geq a\end{cases}$$

Stationary State Equilibrium equations

Uniform density: $T \sim p$; Spitzer resistivity: $\eta \sim p^{-3/2}$

Constant loop voltage: $\eta J \sim (\eta_0 p_0^{3/2})\, p^{-3/2} J \sim V_L$

$$\Longrightarrow \boxed{p = p_0\left[1-(r/a)^2\left(4-6\frac{q_0}{q_a}\right)+(r/a)^4\left(3-6\frac{q_0}{q_a}\right)\right]^{2/3}}, \qquad V_L = B_T\eta_0 p_0^{3/2} / 6q_0R$$

$$\nabla p = \mathbf{J}\times\mathbf{B} \qquad \Longrightarrow \boxed{\frac{1}{2}\frac{d}{dr^2}B_z^2 = \frac{-\dfrac{dp}{dr^2}+\dfrac{B_z^2}{(Rq)^2}\left(1-\dfrac{r^2}{q}\dfrac{dq}{dr^2}\right)}{1+r^2/(Rq)^2}}, \qquad B_z(a) = B_T$$

Stationary pressure profile: $\dfrac{1}{r}\dfrac{d}{dr}\left(r\kappa\dfrac{dp}{dr}\right) = -\eta J^2 = -V_L J$

$$\Longrightarrow \quad \kappa\frac{dp}{dr} = -\frac{V_L B_T}{6q_0R}\frac{1}{r}\int_0^r r\left[1+(r/a)^2\left(-4+6\frac{q_0}{q_a}\right)+(r/a)^4\left(3-6\frac{q_0}{q_a}\right)\right]dr$$

$$\boxed{\kappa = \kappa_0\frac{\left[1-2(r/a)^2\left(1-\dfrac{3}{2}\dfrac{q_0}{q_a}\right)+(r/a)^4\left(1-2\dfrac{q_0}{q_a}\right)\right]\left[1-4(r/a)^2\left(1-\dfrac{3}{2}\dfrac{q_0}{q_a}\right)+3(r/a)^4\left(1-2\dfrac{q_0}{q_a}\right)\right]^{1/3}}{\left[\left(1-\dfrac{3}{2}\dfrac{q_0}{q_a}\right)-\dfrac{3}{2}(r/a)^2\left(1-2\dfrac{q_0}{q_a}\right)\right]}}$$

$$\kappa_0 = \frac{3}{192}V_L B_T a^2 / q_0 R p_0\left(1-\frac{3}{2}\frac{q_0}{q_a}\right) \qquad q_0, q_a, B_T, a, R, \eta_0, p_0 \quad \Longrightarrow \quad V_L, \kappa_0$$

2D Nonlinear Run reaches stationary state

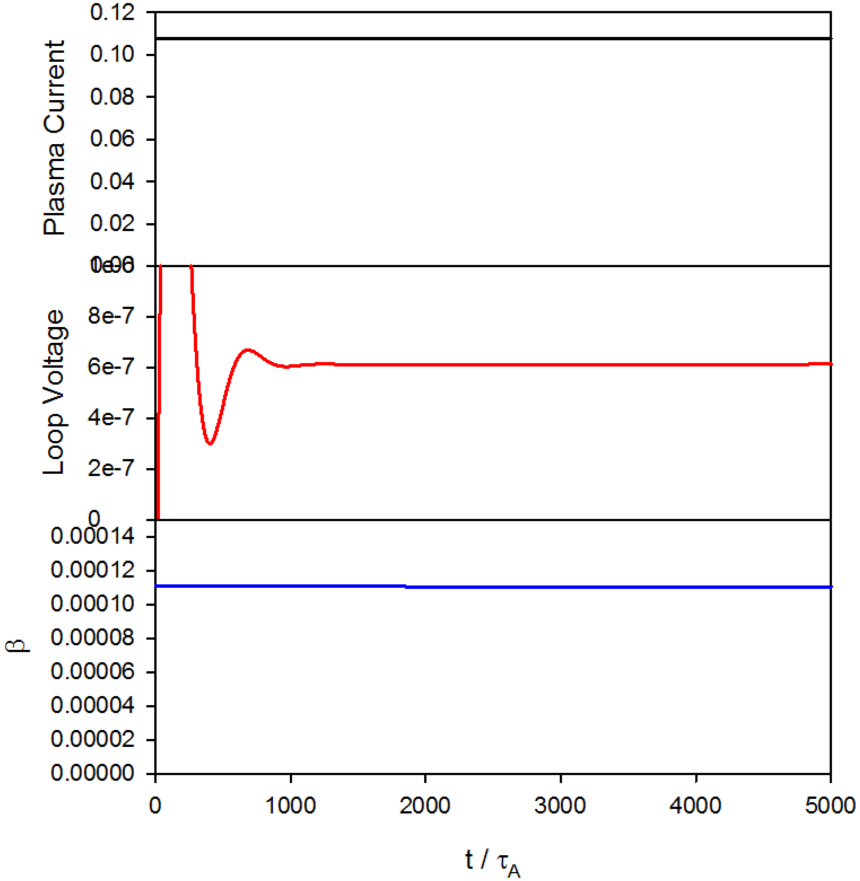

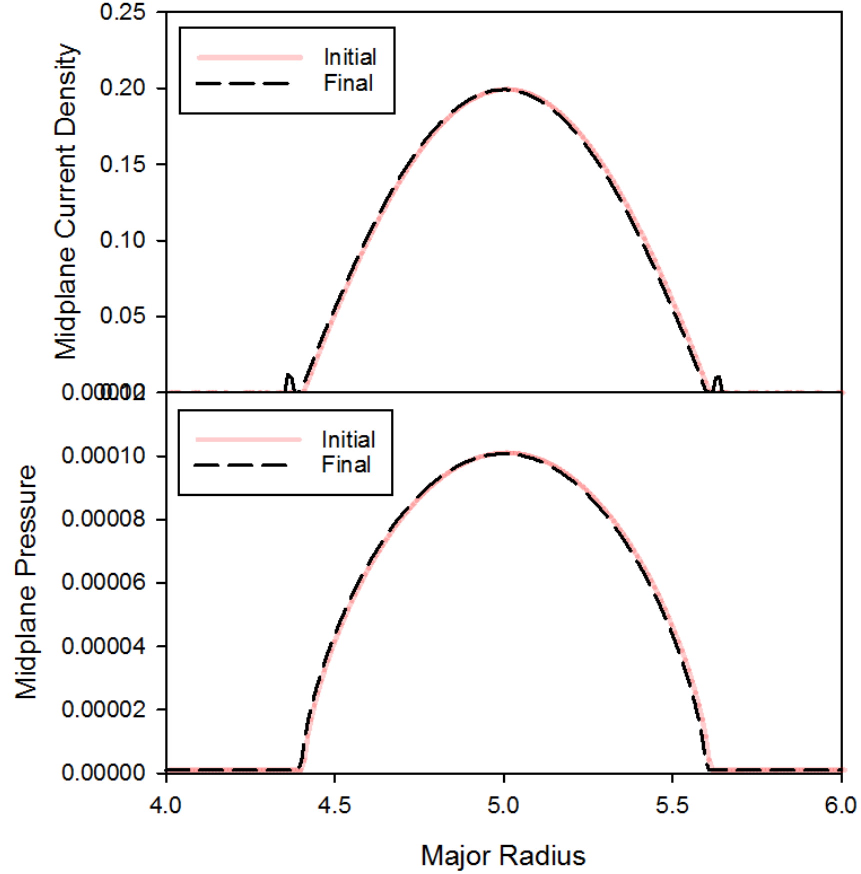

Linear Resistive Stability of Model Cylindrical Equilibrium with no wall (free boundary)

$$q(r)=\begin{cases} q_0\left[1-2(r/a)^2\left(1-\dfrac{3}{2}\dfrac{q_0}{q_a}\right)+(r/a)^4\left(1-2\dfrac{q_0}{q_a}\right)\right]^{-1} & r<a \\ q_a(r/a)^2 & r\geq a \end{cases}$$

q_0

q_a

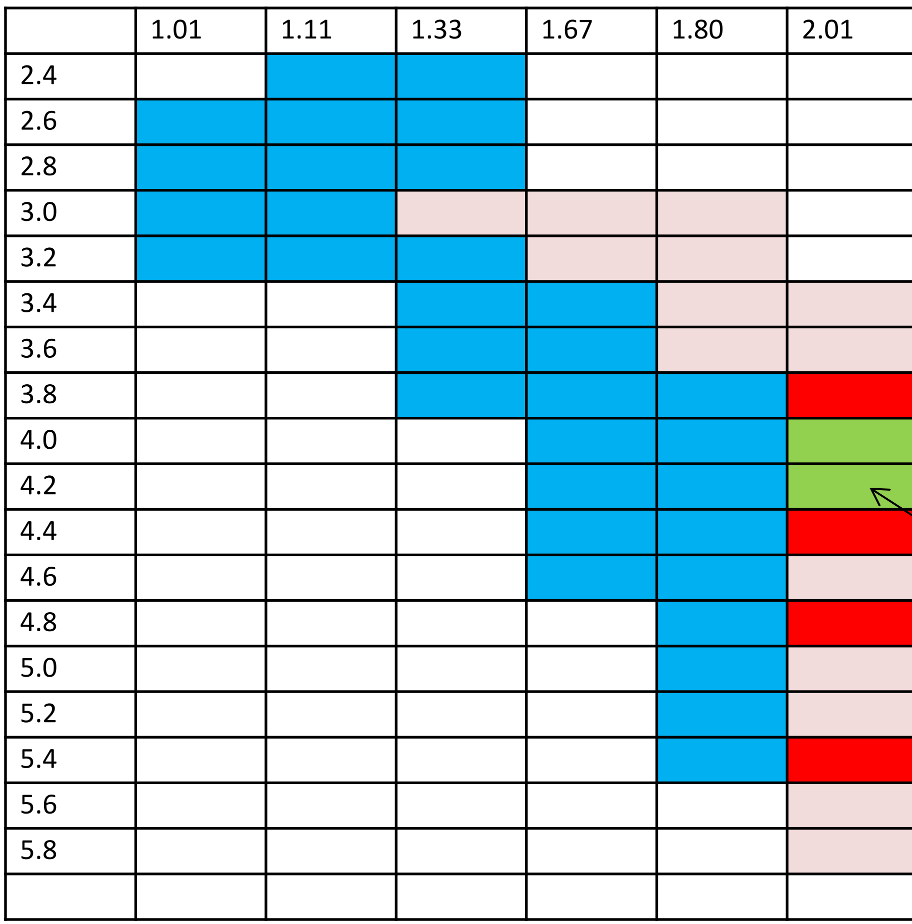

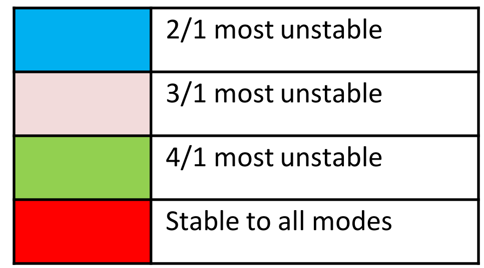

monotonic solutions for:

$$3q_0 > q_a > \frac{3}{2}q_0$$

Examine this case with a nearby wall

Wall at r/a = 0.64: unstable
(4/1) mode dominates

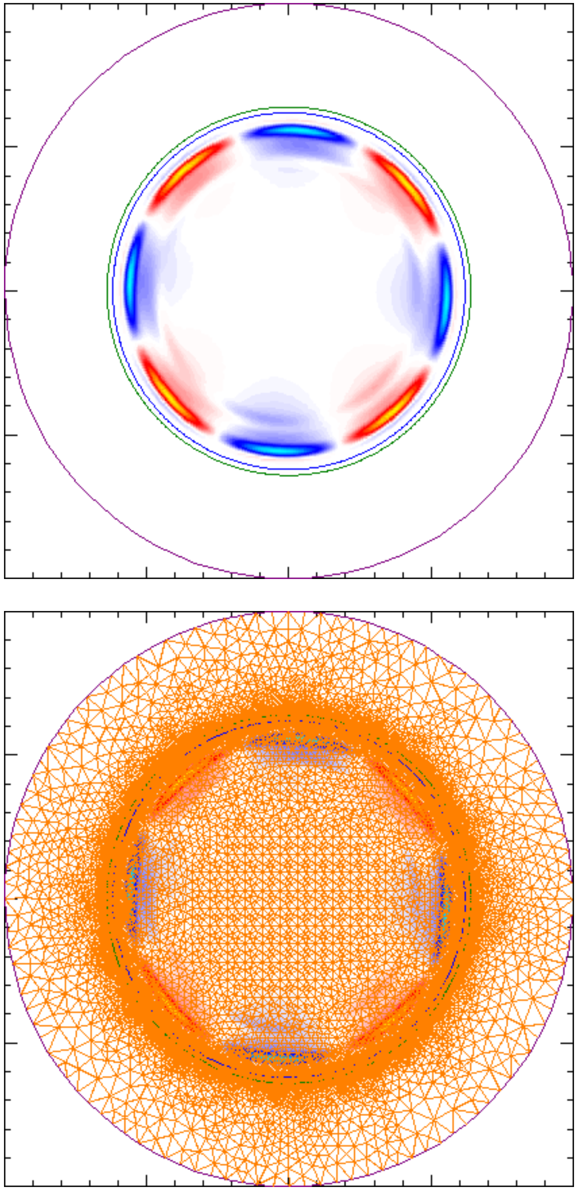

Wall at r/a = 0.62: stable!
(3/1) mode dominates

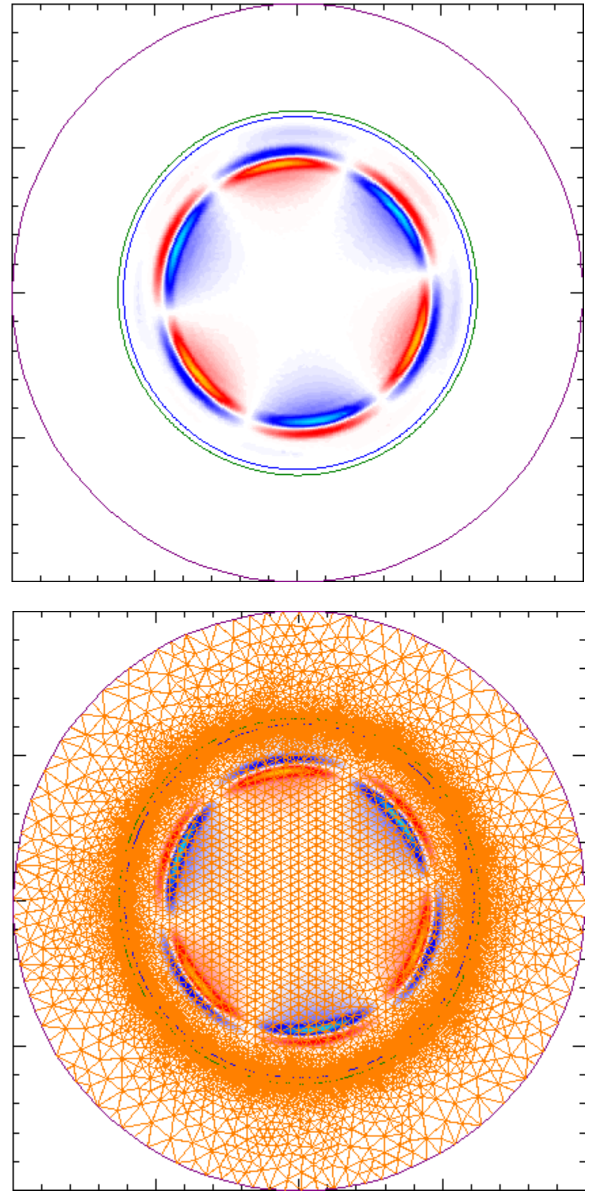

Growth rate of mode depends on wall resistivity

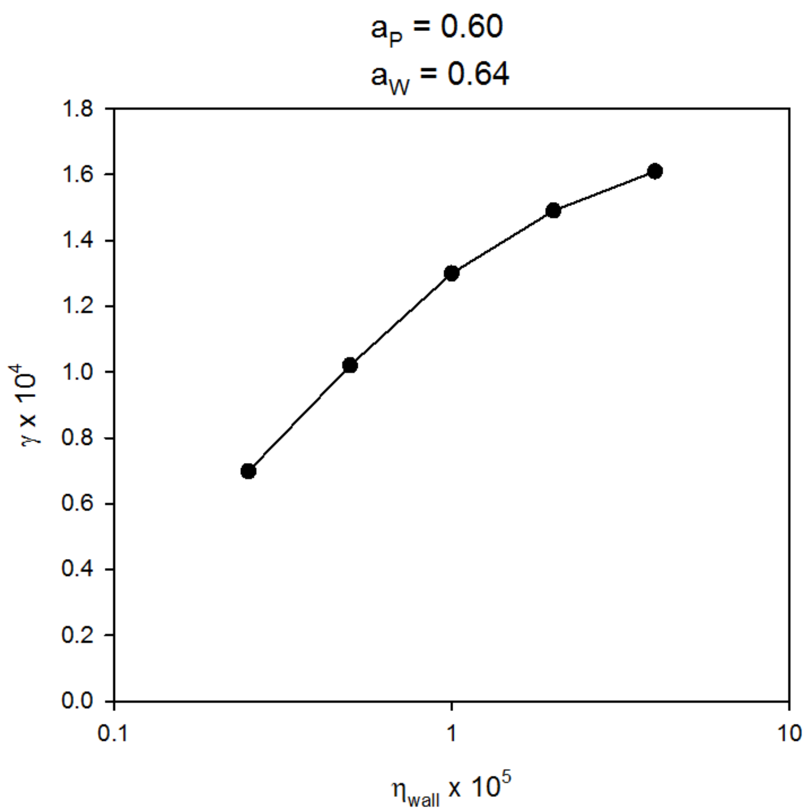

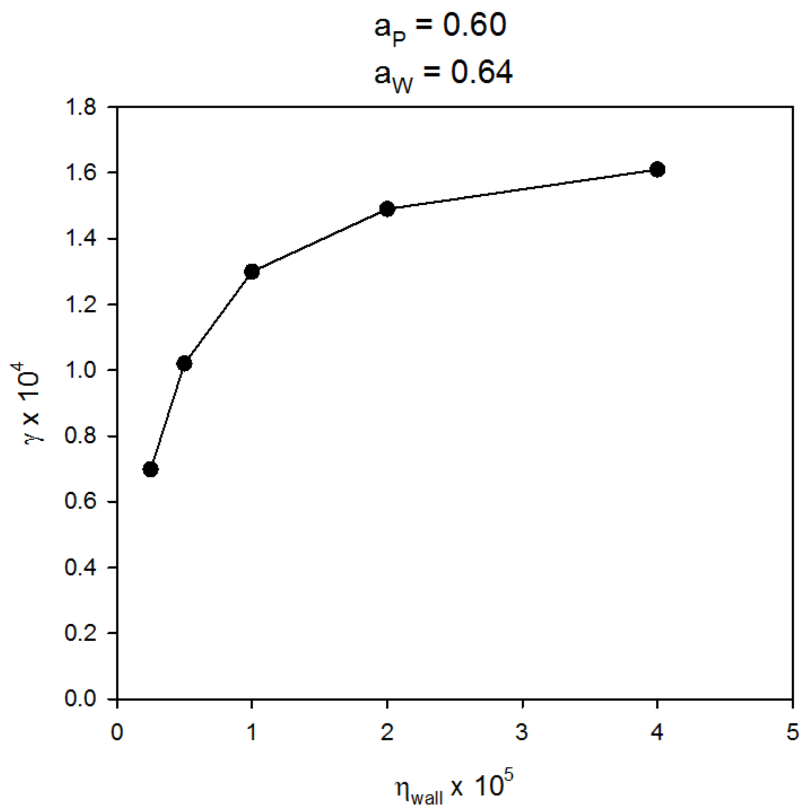

Next Steps

- Add sheared toroidal velocity with torque input (also to equilibrium equation)
- Add error field
- Study interaction of island with resistive wall and error field, and compare with theoretical results for mode locking
- Extend to Torus

References:

[1] Fitzpatrick, R., Nuclear Fusion **33** (1993) p. 1049, Section (3)
[2] Fitzpatrick, R., Nuclear Fusion **33** (1993) p. 1049, Section (6)
[3] Waelbroeck, F. and Fitzpatrick, R. Phys. Rev. Lett. **78** (1997) p. 1703
[4] Fitzpatrick, R., Plasma parameter scaling of the error-field penetration threshold in tokamaks”, Phys. Plasmas, 10 (2003) , p. 1782
[5] Fitzpatrick, R. and Waelbroeck, F. Phys. Plasma. 15, (2008) 012502
[6] Fitzpatrick, R.Plasma Phys. Control. Fusion 54 (2012) 094002.
[7] Reimerdes, H. et al. Nucl. Fusion 49 (2009) 115001
[8] De Bock, M.F.M. et al Nucl. Fusion 48 (2008) 015007 .

7.0 Breakdown of CEMM funding and Workscope by Institution for FY16:

Funding	Institution	PI	Workscope
$ 34 k	GA	Lao/Lyons	RMP and Kinetic MHD in M3D-C1
$ 48 k	GA	Lao/Izzo	Mitigation of disrupting MHD active Plasma
$ 61 k	FTCI	Glasser	Resistive DCON, verification, disruption prediction
$ 62 k	MIT-PSFC	Ramos	Linear kinetic MHD formulation for M3D-C1
$ 62 k	MIT-LNS	Sugiyama	ELM studies with M3D-C1 and benchmarking
$ 62 k	HRS Fusion	Strauss	Disruption studies for forces and benchmarking
$ 176 k	PPPL	Jardin	Sawteeth, hybrid-discharges, disruptions, RMPs, ELMS
$ 43 k	SCOREC RPI	Shephard	Mesh and solver improvements for M3D-C1
$ 166 k	Tech-X	Kruger	EHO, giant sawteeth, NTM, code performance
$ 118 k	Utah State	Held	RSAE benchmark, NTM, giant sawteeth
$ 166 k	U. Wisc.(EP)	Sovinec	Sheath bcs for VDEs, GS collab., ELM topics